SUPPLEMENTAL EXPERIMENTAL PROCEDURES

Fly Strains, culture, and drug treatments

All flies were maintained at 25°C unless otherwise indicated. *fat2*^{58D} and *fat2*^{103C} are gifts from Dr. Christian Dahmann. *UAS-EB1::GFP* is a gift from Nasser Rusan, and *UAS-SpastinEP* is a gift from Nina Tang Sherwood. RNAi strains against the following genes were generated by the Harvard TRiP: *Fat2* (BDSC #40888), *CLASP* (BDSC #34669), *Hem* (BDSC #29406), *Abi (*BDSC #51455*); mCherry* (BDSC #35785) was used as a control. Mild *Fat2* knockdown was achieved using VDRC ID #27113. To temporally control knockdown, *tj-GAL4 tubP-GAL80*^{ts} was crossed to *UAS*-RNAi strains. Adult females were collected at 22° and shifted to 29°. Stage-specific temperature shifts were timed based on duration of stages of ovarian development (Spradling, 1993), informed by the temperature dependence of Drosophila development. To depolymerize microtubules, adult flies were fed with yeast paste mixed with colchicine at 62.5 μg/ml (Sigma); to inhibit Arp2/3 activity, cultured ovarioles were treated with CK-666 at 500 μg/ml (Millipore). All flies were flipped onto fresh yeast daily to ensure no mid-stage follicle degeneration or egg retention.

Microscopy and Immunostaining

Ex vivo follicle culture was performed as previously described (Haigo and Bilder, 2011; Spradling, 1993), with minor modifications. Images were acquired using an inverted Zeiss LSM700 with LD C-Apochromat 40x/NA 1.1 water-immersion lens. Other fluorescent images were acquired with a Zeiss LSM700 using Plan-Apochromat 40x/ NA 1.3 oil-immersion lens. Follicle and egg aspect ratios were calculated from images taken with an AxioImager.M1 (Zeiss) with 10x/NA 0.3 air objective lens; data was analyzed and displayed using GraphPad Prism 6 or Rstudio(Team, 2015) with ggplot2. Figures were assembled in Adobe Illustrator CS6.

Adult ovaries were dissected in PBS or Schneider's Drosophila medium (Gibco) and fixed with 4% formaldehyde in PBS for 15 min and stained as previously described. Stains with TRITC-phalloidin (Sigma) and DAPI (Molecular Probes) were mounted in SlowFade Antifade solution (Invitrogen). The following antibodies were also used: mouse monoclonal anti-acetylated-α-tubulin (1:300, Santa Cruz), and AlexaFluor-488, -563, and -633 conjugated secondary antibodies (1:400, Molecular Probes).

Image analyses and statistics

Follicle rotation velocities were either measured by the displacement of cell nuclei perpendicular to the AP axis, taken at the follicle equator, or plasma membranes stained with 5μg/mL FM4-64FX dye (Molecular Probes). Angular velocity was calculated using measured follicle maximal circumference. 3D Opacity projections were generated with Volocity (Perkin Elmer). Other images were processed in Fiji (Schindelin et al., 2012).

Orientation and alignment of the cytoskeleton was analyzed in fixed ovarioles stained with TRITC-phalloidin and anti-acetylated-tubulin, mounted on concave slides (Ted Pella) to prevent deformation. *in toto* images were collected with confocal microscopy with pixel width of 0.07-0.15 μm and voxel depth of 0.35-0.50 μm.

We used ImSAnE (Heemskerk and Streichan, 2015) to 'unroll' follicles and germaria. In brief, coarse identification of the Surface Of Interest (SOI) is followed by representing the SOI as a smooth mesh, equipped with a coordinate system for mapping to the plane. Images were first rescaled to uniform aspect ratio at the most fine resolution. The ovariole SOI was identified using the basal F-actin signal and the 'ilastik' (Sommer et al., 2011) segmentor interface implemented in ImSAnE, which produced a coarse point cloud. Meshlab (Cignoni et al., 2008) generated a smooth triangulation of

the basal actin layer from the point cloud, following publicly available ImSAnE protocols. The ImSAnE CylinderMeshWrapper class automatically generates a coordinate system embedded in the triangulation for mapping the SOI to the plane: the long axis and azimuth around it are used as a discretized coordinate pair on the surface and the image data interpolated at the corresponding embedding point of each discretized coordinate pixel, generating a planar projection of the data. Image contrast was enhanced with the contrast limited adaptive histogram enhancement (CLAHE) plugin (Fiji). To automatically determine local orientation of actin filaments, region 2 germaria and stage 1 follicles were first screened with a uniform raster of 20x20 px/4 μm^2, overlapping by 2.23 µm; for stage 2 and older, cells were segmented based on cortical actin signal. To determine the polarization axis of basal actin filaments A in boxes or segmented cells, we measured spatial frequency patterns using Fourier's method, from which a nematic order parameter defined as $S = 1/N \sum_{k=1}^{N} e^{2iA}$ was constructed. Orientation to the A-P axis (defined by polar cell position in early follicles, and long axis in germaria and elongated follicles) and the standard deviation (σ) of angles within a follicle were measured using the curvature-corrected dot product of unit vectors with corresponding orientation. Error bars in cytoskeletal alignment analyses represents SEM and statistical significance was assessed by Welch's unequal variances *t*-test. Error bars in charts for rotation velocity (Figure3E, 4C), mature egg aspect ratio (Figure3F, 4D), percentage round eggs (Figure 4E) represent standard deviation. Unless stated otherwise, statistical significance was assessed by Welch's unequal variances *t*-test.

EB1-GFP comet tracking

tj>UAS-EB1:GFP flies were raised on yeast for 5 days at 29° C, flipped onto fresh yeast for 6-12 hours. Ovarioles were dissected in modified Schneider's medium and mounted using low-melting point agar. Movies of basal EB1 comet growth were made on the Zeiss LSM700 with LD C-Apochromat 40x/NA 1.1 water-immersion lens. Individual EB1 comets were tracked manually in Fiji by generating kymographs perpendicular to the AP axis of the germarium and measuring the slope of EB1:GFP comet growth. Microtubule growth bias was calculated by the formula |(D-S)/T| where D equals the number of dextral comets, S equals the number of sinistral comets and T is the total number of comets. Statistical significance was assessed by Unpaired T-test.

SUPPLEMENTAL FIGURE LEGENDS

Supplemental Fig. 1: Early stages of follicle development (related to Fig. 1)
(A) Confocal section of anterior ovariole, stained for DNA (blue), F-actin (red) and acetylated tubulin (green). **(B)** Diagram of germarium and st. 2 follicle, showing position of stem cells, somatic and germline cells, and stalk cells.

Supplemental Fig. 2: Arp2/3 regulators are required for egg elongation (related to Fig. 3)
Knockdown of Arp2/3 regulators *Hem* **(A)** and *Abi* **(B)** by *tjGAL4 UAS-RNAi* in genetic screen produces round eggs; aspect ratios are quantitated in **(C)**.

Supplemental Fig. 3: Characterization of *fat2 RNAi* phenotype (related to Fig. 4)
(A) Aspect ratio and **(B)** st. 7 actin alignment of *fat2* null mutant vs *tj>fat2 RNAi* follicles demonstrates effective depletion of *fat2* function by RNAi.

Supplemental Movie S1, related to Fig. 1: Live imaging of ovariole (genotype: *vkgGFP, His2aVmRFP*) shows rotation commencing as follicle buds at st. 2.

Supplemental Movie S2, related to Fig. 4: Live imaging of *fat2*-depeleted ovariole (genotype:*tj>fat2 RNAi; vkgGFP, His2aVmRFP*) shows failure to initiate rotation.

Supplemental Movie S3, related to Fig. 4: EB1-GFP comet imaging in the germarium.

Supplemental Movie S4, related to Fig. 4: Imaging of EB1-GFP stage 1-2 follicle during the initiation of rotation. MT growth bias for this follicle is 0.48 sinistral at st 1.

SUPPLEMENTAL REFERENCES

Cignoni, P., Callieri, M., Corsini, M., Dellepiane, M., Ganovelli, F., and Ranzuglia, G. (2008). MeshLab: an Open-Source Mesh Processing Tool. Eurographics Italian Chapter Conference.

Haigo, S.L., and Bilder, D. (2011). Global tissue revolutions in a morphogenetic movement controlling elongation. Science *331*, 1071–1074.

Heemskerk, I.J., and Streichan, S.J. (2015). Developmental cartography: Compressing Bio-Image Data by Dimensional Reduction. Nature Methods.

Schindelin, J., Arganda-Carreras, I., Frise, E., Kaynig, V., Longair, M., Pietzsch, T., Preibisch, S., Rueden, C., Saalfeld, S., Schmid, B., et al. (2012). Fiji: an open-source platform for biological-image analysis. Nat. Methods *9*, 676–682.

Sommer, C., Straehle, C., Kothe, U., and Hamprecht, F.A. (2011). ilastik: Interactive Learning and Segmentation Toolkit. pp. 230–233.

Spradling, A.C. (1993). Developmental genetics of oogenesis. In The Development of Drosophila Melanogaster, M. Bate, and A. Martinez Arias, eds. (New York: CSHL Press), pp. 1–70.

R Team (2015). RStudio: Integrated Development for R. Www.Rstudio.com.

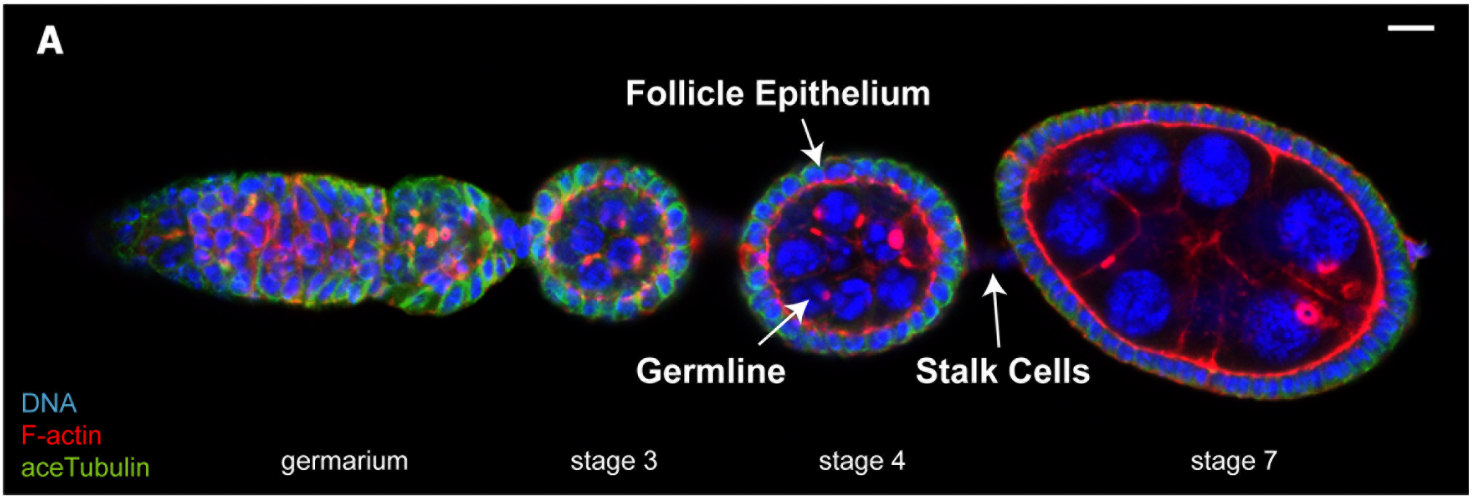

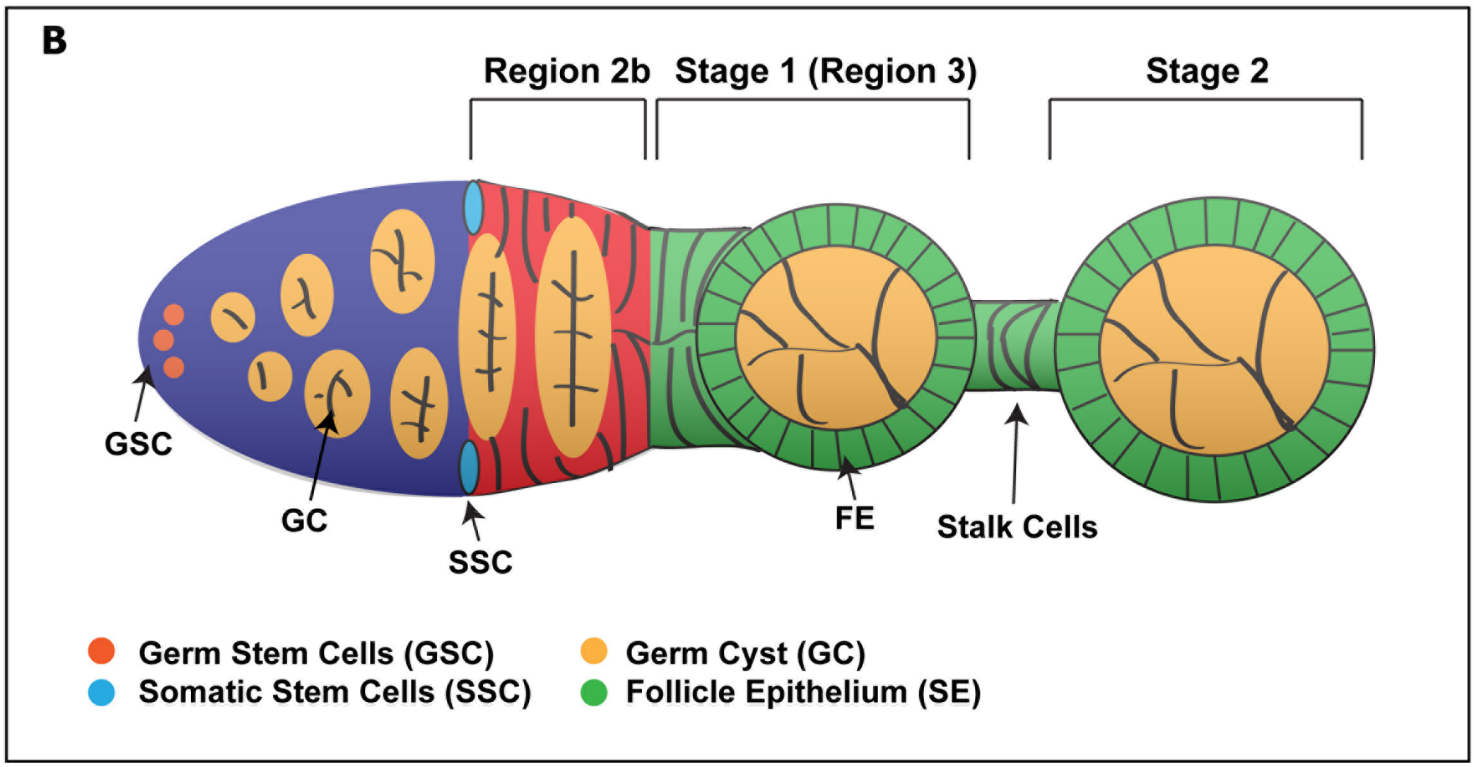

Supplemental Figure 1

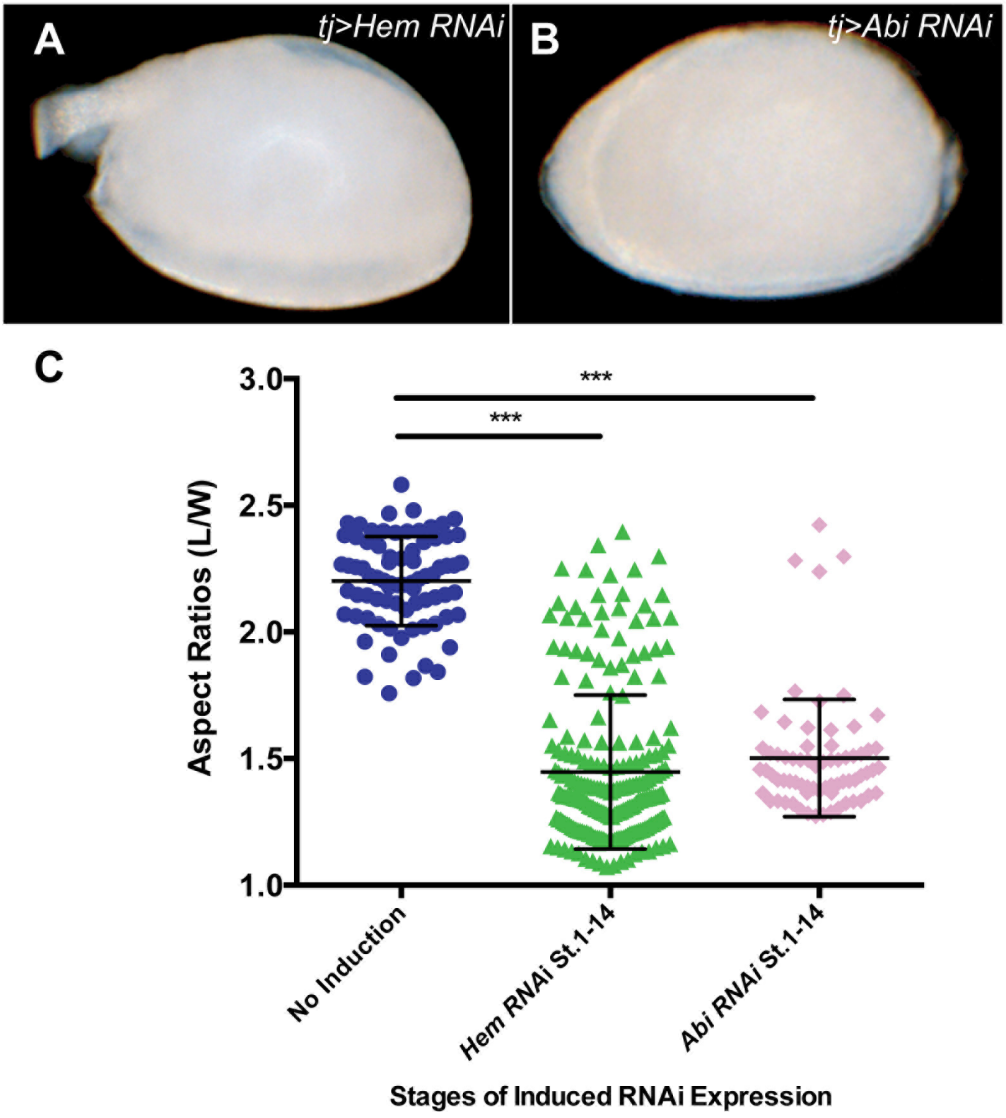

Supplemental Figure 2

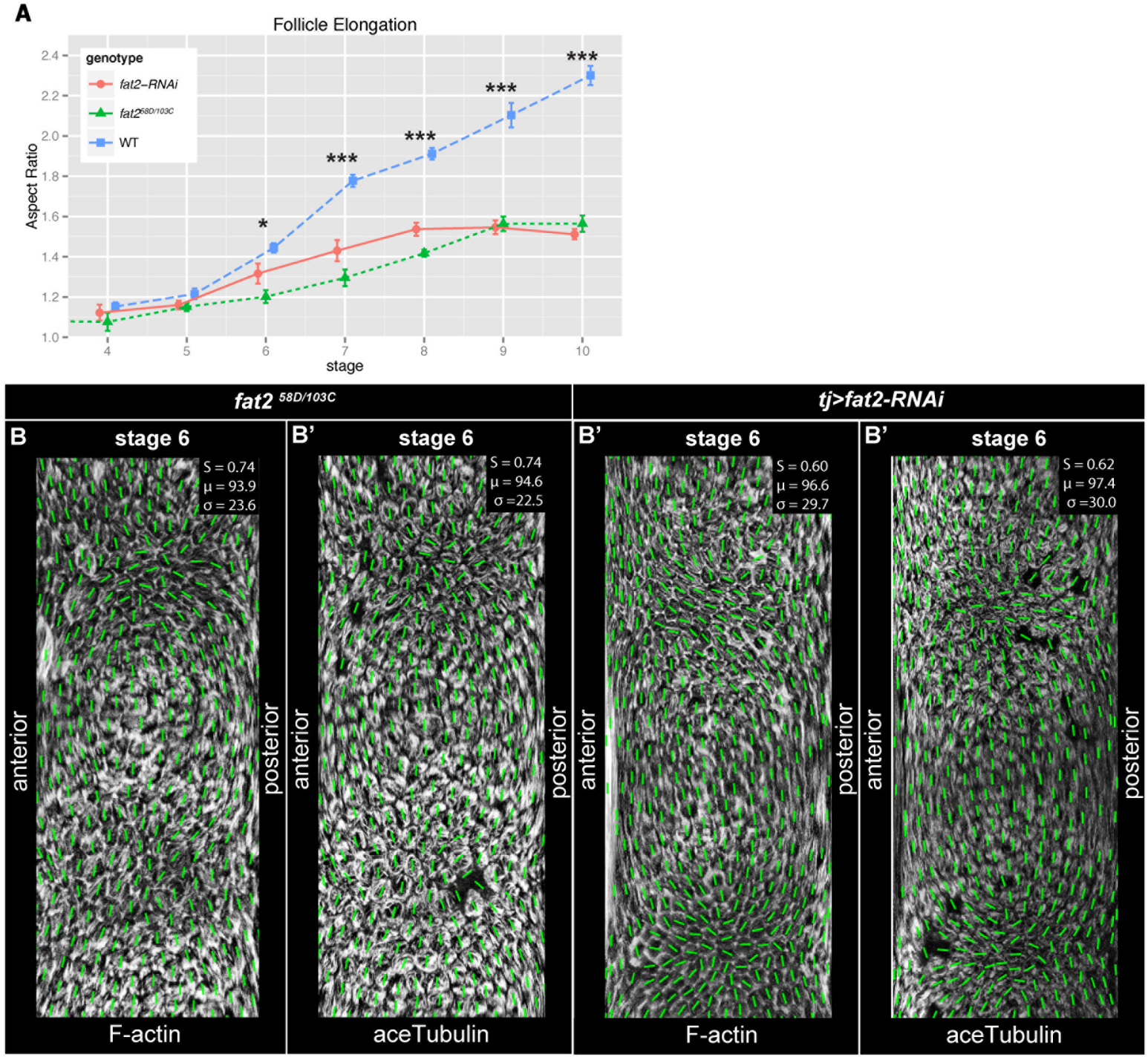

Supplemental Figure 3